Numerical Weather Prediction

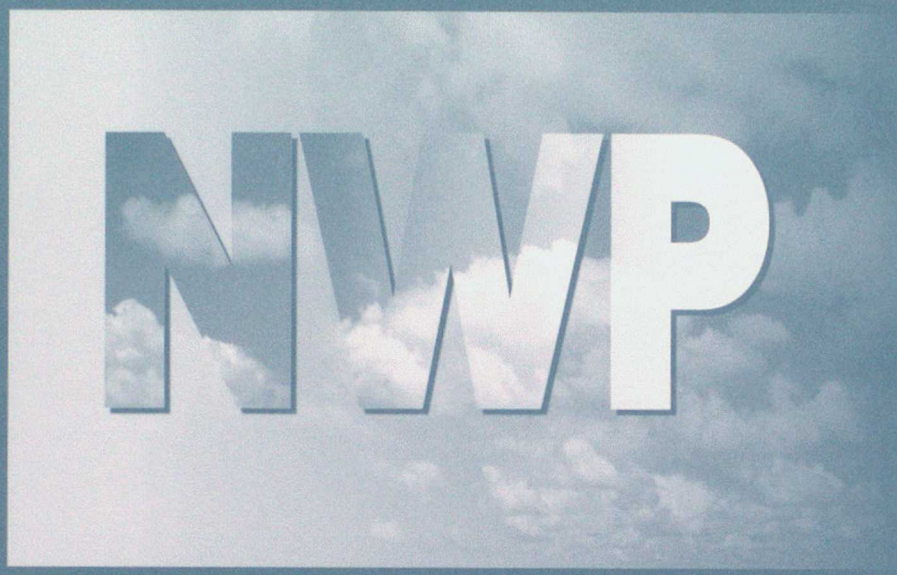

Forecasting Research Technical Report No. 356

Diagnosing Error Sources in Extratropical Cyclone Lifecycles

June 2001

D.R. Cameron and S.F. Milton

Met Office , NWP Division , Room 344 , London Road , Bracknell , Berkshire ,RG12 2SZ, United Kingdom

Numerical Weather Prediction
Technical Report No. 356

Diagnosing Error Sources in Extratropical Cyclone Lifecycles

D. R. Cameron and S. F. Milton
NWP Division

June 2001

The Met Office
NWP Division
Room 344
London Road
Bracknell
Berkshire
RG12 2SZ
United Kingdom

Tel: 44(0)1344 856245 Fax: 44(0)1344 854026 e-mail: john.armstrong@metoffice.com

Abstract

This report uses both time mean and case by case methods to assess the systematic error in extratropical cyclone lifecycles in the Atlantic Stormtrack for operational forecasts during the period September 1998 to Febuary 1999. It is found that the main area of forecast variability is shifted too far east relative to the analysis and that individual systems deepen too slowly in the western Atlantic and fill too slowly in the eastern Atlantic. The report goes on to look at a case study of a 5 day forecast from 15th November 1998 which fails to capture the main cyclogenesis. PV analysis and transplant experiments suggest that deficiencies in the upper level PV at day 3 of the forecast are crucial to the poor cyclogenesis. Lagrangian trajectories and a PV budget analysis are used to show that horizontal diffusion is responsible for a drop in upper level PV as the flow passes over America prior to day 3 of the forecast. Finally a sensitivity experiment with ∇^6 diffusion confirms that the lack of scale selectivity of the horizontal diffusion is important for the poor cyclogensis in the case study considered. It is suggested that many of the diagnostic techniques used in this study could be helpful in subsequent systematic error studies.

Contents

1 Introduction

The accurate prediction of extratropical cyclones beyond day 3 remains a continuing challenge for operational NWP centres. Although on many occasions the current generation of NWP models display an impressive ability to predict explosive cyclogenesis events, careful examination of model performance highlights some remaining deficiencies in simulating the lifecycles of extratropical cyclones. Failure to accurately predict extratropical cyclones beyond day 3 may be attributed to inaccurate initial conditions (Rabier *et al* (1996)), inadequate resolution, errors in modelling subgridscale parametrised physics, or combinations of all of these factors (Anthes (1983)). In this paper we discuss possible "systematic" deficiencies in the lifecycle of extratropical cyclones in the Atlantic Stormtrack for the Operational Unified Model during 1998-1999. Although the original motivation of this study is to examine systematic error, this paper also highlights some general diagnostic techniques which could be useful in other systematic error studies.

2 Data and Model Formulation

For this study we consider operational global UM forecasts for 181 days covering September 1998 to February 1999. The version of the model operational during this period had a resolution of 0.55 degrees latitude by 0.833 degrees longitude ($\approx$ 60km grid spacing in mid-latitudes) and thirty hybrid levels in the vertical. The model physics include, gravity wave drag, orographic roughness (form drag), fully interactive radiation, prognostic cloud liquid water and ice, turbulent mixing based on eddy diffusivity, massflux convective parametrization including momentum transports and CAPE based closure. The assimilation scheme is a nudging based scheme called the analysis correction scheme, operational prior to the introduction of 3D variational assimilation scheme in March 1999.

3 Systematic errors in the Atlantic Stormtrack

a Time mean errors

Figure 1 shows the time averaged mean sea level pressure (MSLP) field for the Met Office analyses, T+120 hour forecasts and the T+120 mean forecast error. The analysis shows the characteristic Icelandic low of 1000hPa at 60N and the Azores high of 1024hPa at 35N with south-westerly flow at 45N. The mean error (figure 1(c)) shows pressure to be too high in the west Atlantic and too low in the east Atlantic. This error pattern reflects an eastward shift and a reduction in depth of the forecast Icelandic low (figure 1(b)). We also note a tendency of the model to weaken the westerly flow in the west Atlantic and increase westerly flow over Europe. Also shown is the standard deviation of the errors (figure 1(d)) which represents the "random" error component. This shows maxima of between 10-12 hPa oriented from SW to NE along the path of the stormtrack. The ratio of these two error variances (systematic and random) to the total error variance shows that the systematic error only accounts for 10% of the total error variance. However, the systematic error component of individual systems may be larger when considering a Lagrangian (e.g cyclone tracking) rather than Eulerian statistic.

To investigate the role of individual synoptic systems in these time mean errors we have composited the T+120 mean errors at each gridpoint into 5 categories according to the value

of the analysed pressure (1= less than 990hPa, 2= 990-1000, 3= 1000-1010, 4= 1010-1020, 5= greater than 1020). Figure 2 shows the composite mean errors for the category 1 (deep Lows) and categories 2 and 3 combined (shallow lows). The errors in category 1 ($P < 990hPa$) suggest that on average the T+120 forecasts of pressures below 990hpa are not deep enough (figure 2(a)). This error accounts for approximately 75% of the total mean error between Iceland and Greenland. In contrast, the mean error of categories 2 and 3 has pressures too high in the west Atlantic and too low to the east (figure 2(b)). The error in the east Atlantic contributes to the negative errors in the total mean error (figure 1(c)). The negative total mean error over Scandinavia, (figure 1(c)) can be attributed to the existence of blocking anticyclones in the analysis (category 5 - not shown) which are underpredicted in the forecasts.

These composite errors suggest that deep cyclones are underpredicted and cyclones of intermediate depth are underpredicted in the west Atlantic but overpredicted in the east. However, compositing the mean error in this way by analysis may be flawed as it takes no account of occasions when deep lows are forecast but not observed. Therefore, we should also consider the frequency distribution of the analysis and the forecast to see if the overall climatology of deep lows is correct. This is done in figure 3 which shows the frequency of occurence of cyclone central pressures lower than 990hPa for the analysis and forecast. The analyses have a maximum of 30% between Iceland and Greenland which gradually dereases towards Europe (figure 3(a)). The T+120 forecasts have a maxima to the north of the UK (figure 3(b)) which is coincident with the negative errors in figures 1(c) and 2(b). The forecast frequency between Iceland and Greenland is approximately half those in the analysis. Thus these marginal distributions appear to be consistant with the results from the composite errors that the main forecast variability is shifted too far eastward relative to the analysis.

b Case Studies

In order to gain insight into the errors present on a case by case basis we consider some individual case studies. Figure 4 shows central pressures of 3 Atlantic cyclone lifecycles which occurred in quick succession between 17 and 30 November and involved cyclones of 961, 958, and 954 hPa. The depths of the cyclones in the analysis and at succesive forecast ranges are calculated from an objective cyclone tracking program (Terry and Atlas (1996)). In all 3 cases the deepest central pressures are underestimated in the model by between 10 and 20 hPa at T+96 and T+120 forecast ranges. The errors prior to the rapid deepening are typically much smaller even at T+120. The forecasts up to T+72 are generally more accurate and the final case study shows very successful forecasts of the 954 low pressure for T+24, 48 and 72 hour forecasts. In the last two cases the forecasts at all time ranges fail to fill sufficiently as the analysed system decays. This is typically when the low system is in the east Atlantic, and agrees with the time mean diagnostics in figures 2(b) and 3(b).

From these diagnostics we gain a picture of the forecast lifecycle beyond day 3 in which deep cyclonic systems are underpredicted in the west Atlantic and in the east Atlantic the cyclones are generally too deep and fail to decay rapidly enough.

4 A Case Study with Poor Forecast Cyclogenesis

The forecast to be considered is one of the cases shown in figure 4(a) and was the forecast that started at 12z on 15th November 1998. Figure 4(a) shows that on the 18th of November, after 3 days of the forecast, the central pressure of the extratropical cyclone, marked by a diamond, was in reasonable agreement with the analysis. However, by the 19th, one day later, the central pressure of the analysed cyclone was far deeper than the T+96 forecast (marked by a cross). This error continues through the forecast, so that after 5 days the central pressure of the forecast cyclone at T+120 (open square), was severely underdeveloped by over 20hPa relative to the analysis.

Figure 5 shows the mslp pressure charts for days 3 to 5 of this forecast. The cyclone in question is just off the east coast of America at day 3 and subsequently moves north and east into the Mid-Atlantic and develops. At day 3 the structure and depth of the forecast cyclone is relatively good although, there is a slight positional error. As discussed above, the discrepancy between the forecast and the analysis only really becomes apparent between days 3 and 4 of the forecast, as the cyclone moves north and east. Although the position of the forecast cyclone at day 4 is relatively good there is now a very clear discrepancy in structure and depth of the analysed and forecast cyclones. After 5 days the forecast cyclone centred between Greenland and Iceland is almost 30hPa in error and in particular, the strong flow over Scotland is severely underdeveloped.

a PV Analysis

Hoskins *et al* (1985) use the PV framework to present a conceptual model of frictionless and adiabatic cyclogenesis in which an upper level cyclonic PV anomaly with vertical motion ahead of it, moves over a low level PV anomaly induced by warm boundary layer air. The two anomalies phase lock and their cyclonic circulations reinforce each other leading to development of the system. Diabatic heating associated with latent heating in the region of ascent can also significantly enhance the cyclonic system. Mid tropospheric heating implies a flux of PV from the upper to the lower troposhere enhancing the low level circulation (see Stoelinga (1996) for a numerical case study). From this conceptual model we can see it is important that an NWP model maintains an accurate climatology of both upper level PV anomalies and warm (and moist) boundary layer air in order that cyclogenesis events are predicted with the correct frequency and intensity.

In this section we use this conceptual PV approach in order to help diagnose possible reasons for the poor development of the forecast cyclone after day 3 described above. Shown in figure 6 is upper tropospheric (315K) Ertel PV and lower tropospheric (850hPa) PV for days 3 and 4 of the forecast with the corresponding analysis. The difference between the lower tropospheric PV values of the forecast and the analysis at day 3 are relatively small (figure 6(a) and (b)) when compared to the differences at day 4 (figure 6(c) and (d)), which is in agreement with what was observed in mslp charts discussed above. However, the analysed upper tropospheric Ertel PV, at 42N 62W on day 3, is greater by $\approx$1PVU than the forecast PV although, the position of the forecast PV feature is relatively good. By day 4 the analysed upper and lower level PV anomalies are both growing and from vertical cross-sections (not shown) appear to have phase locked however, the forecast chart at day 4 is quite different. The lower troposheric PV feature has moved north away from the upper tropospheric PV anomaly which appears to have decreased by $\approx$1PVU. Therefore, one hypothesis is that the lack of development in the forecast cyclone is

related to the deficiency in the upper tropospheric PV anomaly off the east coast of America at day 3 of the forecast.

b PV Transplant Experiments

In order to test the assertion made in the previous section, experiments have been conducted where the upper level PV of the forecast and analysis at day 3 has been altered and the forecast has been run on from that point in order to assess the impact on the subsequent cyclonic development. These experiments are summarised in table below and shown in figure 7.

Experiment	Description	Central Pressure of Cyclone
CTL120	Control T+120 forecast from 15/11/98 verifying on 20/11/98	989hPa
TRA120	T+120 forecast from 15/11/98 verifying on 20/11/98 with PV transplant at upper levels from analysis at day 3 (18/11/98)	967hPa
CTL48	Control T+48 forecast from 18/11/98 verifying on 20/11/98	968hPa
TRF48	T+48 forecast from 18/11/98 verifying on 20/11/98 with PV transplant at upper levels from day 3 of CTL120 forecast.	986hPa

The first entry in the table above (CTL120) is the five day forecast from the 15th Nov. 1998 verifying on the 20th Nov. 1998 that has already been discussed. By day 5 it has a central pressure of 989hPa (figure 7(c)) which compares poorly with the analysed cyclone (figure 7(a),961hPa). For the purposes of this experiment this 5 day forecast will be considered as the control 5 day forecast.

The second entry in the table (TRA120) is also a 5 day forecast starting at 15/11/98 and verifying on 20/11/98. In this case the integration is stopped after 3 days and the upper level PV from an analysis for that day (figure 6(a)) is transplanted into the forecast. In practise this is done by transplanting analysis winds and temperatures from 12z on the 18/11/98 into the forecast above level 10, (approx 500hPa) and reconfiguring. The model is then run on for a further 2 days, with the new upper level PV, to see if there is an impact on the cyclone development. The mslp chart for this experiment (TRA120) is shown in figure 7(b). The central pressure of the forecast cyclone is now 967hPa which is a significant improvement over the control (CTL120) and is considerably closer to the depth of the verifying analysis (figure 7(a),961). Clearly, giving the forecast the analysed upper level PV at day 3, before the explosive development, has had a beneficial impact on the subsequent forecast.

The above experiment does support the assertion that the upper level PV at day 3 is of crucial importance to the subsequent development. However, as a further test we aim to "degrade" the day 3 analysis (12z 18/11/98) by transplanting the upper level PV at day 3 from the poor 5 day forecast (CTL120, figure 6(b)). We then run the model for two days, verifying as before on 20/11/98, to see the effect on the subsequent cyclogenesis. This experiment is the entry (TRF48) in the table above and is compared against a T+48 control forecast (CTL48), from the unaltered day 3 analysis, which also verifies on 20/11/98. The central pressure of the integration with the "degraded" analysis (figure 7(d), 986hPa) TRF48 is clearly significantly higher

than the control forecast (figure 7(e), 968hPa) CTL48. Indeed the depth of the cyclone in the T+48 forecast with the "degraded" analysis (TRF48) is not much better than the original T+120 forecast (CTL120).

Other experiments (which are not shown here) have been run where the lower tropospheric winds and temperatures from the analysis at day 3 have been transplanted into forecast. As was done for the upper level PV experiments described above. But this was found to have little or no effect on the poor development of the subsequently forecast cyclone.

The results from these PV transplant experiments confirm the assertion made in the previous section that it is the difference in the upper level PV between the forecast and the analysis at day 3 that is crucial for the difference in the subsequent cyclogenesis at days 4 and 5.

c Lagrangian Trajectories

In order to determine why the upper level forecast PV has been reduced after 72 hours, it is useful to determine where and when the change in the forecast PV occurs. We therefore turn to a Lagrangian method of tracking individual air parcels through the forecast and analysis. This has been done using an offline trajectory program written by Methven (1997). The method involves interpolating model wind data onto a cluster of predefined particles at time zero. The number of particles to be used and their positions are chosen as desired. The next wind record in the sequence is now read in and the position of each particle is integrated between the two wind records (forward or backward) to produce forward or backward trajectories. This is done by interpolating the winds in space and time to the particle's position and using a fourth order Runge-Kutta "integrator" scheme. Various diagnostic attributes can be assigned to each particle (eg temperature, PV) by interpolating the selected attribute field onto the particle's position. Thus it can be noted how each of these attributes vary throughout the trajectories of the particles. Subsequent wind records are read in and the process is repeated until the trajectories reach their desired length.

We are interested in the evolution of the cluster of air parcels that end up in the region of the upper level PV anomaly centred at 42N 62W (figure 6(a)). Therefore, a set of particles is released in this region (figure 8(a)), for the analysis on the 18th of November, which corresponds to the third day of the forecast. We then perform a three day back trajectory, on the 6 hourly analysis wind data, to see where this anomalously high PV air came from. An approach similar to that of Wernli and Davies (1997) is used to pick out a coherent ensemble of trajectories that describe the Lagrangian advection of day 3 PV anomaly we are interested in. The particles are released at 400hPa and only those particles which have PVU greater than 1, at initial time (12z 18/11/98) are considered. The back trajectories of these particles, suggests that many of the high PV particles come from a similar geographical region centred near 150W (figure 9) and that this high PV air is decending from the lower stratosphere $\approx$ 250hPa (height plot not shown). Indeed if one looks at 315K Ertel PV for the initial analysis time (15th Nov. figure 8(b)) we see a significant anomaly, greater than 8 PVU, centred on the region that we would expect from the trajectories. The trajectories show that this high PV air then tracks across America over the Great Lakes to end up on the eastern seaboard where the rapid cyclogenesis begins.

Forward trajectories are now calculated from particles that are released at 12z on the 15th November 1998 which is Day 0 of the forecast. The particles are released at 250hPa from

the initial anomalous high PV area found from the back trajectories above (figure 8(b)) and integrated for three days in order to see what happens to this high PV air in the forecast and analysis. Initially we calculate the forward trajectories for the analysis winds. This time we select only those analysis particles which end up in the region near 42N 62W after 3 days (figure 8(a)). This being the region where we find the discrepancy in the upper level PV between the forecast and analysis that we believe is crucial for the subsequent rapid development. We now calculate the forward trajectories for the forecast winds. In order to make a direct comparison with the analysis trajectories already calculated, we only consider those forecast particles that start from same point as the analysis particles selected above. If one compares the analysis and forecast PV for these forward trajectories, we can see some significant differences (figure 10). There is variation in the PV along the trajectories of both the analysis and the forecast. This suggests that either there are real non-conservative processes acting on the particles as they cross America or possible errors in the trajectory program. Although, the drop in PV of the forecast is far more dramatic than that for the analysis and seems to occur at approximately 2 days after the forecast has begun. It is this loss in PV of the forecast that is apparently crucial for the weak development that occurs later on in the forecast.

d PV Budget Analysis

The Lagrangian trajectory study above suggests that for this case of poor cyclogenesis there is a crucial drop in upper level PV after 2 days of the forecast. So the question remains as to why this dramatic drop in the upper level PV has occurred as the flow crossed America. In order to help answer this question we use a PV budget approach similar to that used by Klinker (1994), Stoelinga (1996) and Wirth and Egger (1999), where we use the PV budget equation (Hoskins *et al* (1985) (shown below)) in order calculate the sources and the sinks of PV from each routine of the model every 6 hours of the forecast. The term on the left hand side of the equation below is the Lagrangian derivative of total Ertel PV. If the Ertel PV is conserved following the motion of the fluid then this term equals zero. Therefore the terms on the right hand side of the equation represent sources and sinks of Ertel PV. The first term on the right hand side is the contribution to PV from diabatic processes and the second term represents changes in PV from frictional processes.

$$\frac{DP_V}{Dt} = \frac{\zeta}{\rho} \cdot \nabla\dot{\theta} + \frac{\nabla\theta}{\rho} \cdot \nabla \times F$$

In practise this PV budget analysis is done by calculating the contribution to the wind and/or temperature by each routine in the model (eg convection or advection) at each timestep. A 6 hour mean increment is then calculated, every 6 hours and the above equation is formed in order to calculate the incremental change to the PV per day from each routine. In addition all the contributions from all the routines can be added together in order to obtain the total change to PV per day for that 6 hour period. Contributions to the diabatic part of the PV budget come from radiation (SW and LW), Large-scale and convective precipitation, latent heating and boundary layer processes. Whereas the contributions to the frictional part of the PV budget come from horizontal and vertical diffusion, convective momentum, gravity wave drag and the contribution from the boundary layer turbulent fluxes.

Shown in figure 11(a) and (b) is upper level PV for the analysis and the forecast after 42 hours. The PV structure that we saw at the start of the forecast period (figure 8(b)) has now advected westwards across to the Great Lakes and has been stretched out into a relatively narrow PV feature. It is clear that the forecast PV feature (figure 11(b)) is condsiderably smoother and

weaker than that for the analysis (figure 11(a)) at this time, and it is suggested that this is the same discrepancy in PV that was seen in the trajectory study above. We can now employ the PV budget approach described above to see how the diabatic and frictional source/sink terms have changed the Ertel PV over the previous 6 hours. Shown in figure 11(c) is the total Lagrangian derivative of PV on the 300hPa surface (ie the left hand side of the above equation). We can see how $\frac{DP_V}{Dt}$ has acted to smooth and broaden the forecast PV for the 6 hours previous to figure 11(b). Shown in figures 11(d)-(h) are the five largest diabatic and frictional terms (right hand side of the PV budget equation) that make up $\frac{DP_V}{Dt}$. Although there are significant contributions from convective momentum, LW radiation, convection and latent heating especially off the SE coast of America which is associated with a low pressure system moving up from the subtropics, by far the largest term, in region of interest to the west of the Great Lakes, is from horizontal diffusion. As the PV anomaly is advected across America it is stretched out into a long streamer, giving rise to large gradients of PV over a relatively small area. The scale of the PV becomes small enough that horizontal diffusion acts to remove the tight gradients present and this causes an overall drop in PV relative to the analysis. Therefore, it is the assertion from this PV budget study that it is the lack of scale selectivity of the horizontal diffusion that causes the drop in upper level PV, which contributes towards the poor cyclogensis later in the forecast.

Whilst the contribution to the PV budget from horizontal diffusion is clearly dominant for PV structure (situated in NW America) that we are interested in, it is also instructive to examine PV budget contributions to the low pressure system situated off SE coast of America where other terms in the PV budget appear to be more important. Heating due to the low pressure system will act to distort the θ surfaces such that $\nabla\theta$ will decrease above the heating and increase below the heating. Thus from the PV budget equation we expect upper level PV due to the heating terms to decrease in time which is what we see in figures 11(g) and (h). Radiative cooling above the same low pressure system will act to distort the θ surfaces in the opposite sense to the heating. So we would expect a positive contribution to the PV budget from LW radiation, in the vicinity of the low pressure system, which is what is seen in figure 11(f).

e *Sensitivity of Cyclogenesis to Horizontal Diffusion*

The current operational model at the Met Office uses a horizontal diffusion of $\approx 1hr\nabla^4$. In order to test the assertion made above that the lack of scale selectively of diffusion contributed to the poor forecast of cyclogenesis, we have performed a sensitivity test with diffusion set to $\approx 4hr\nabla^6$ for the 5 day forecast from the 15th November 1998. Shown in figure 12(a) ,(b) and (c) is the mslp for the analysis on the 20th Nov., the 5 day forecast with diffusion of $\approx 1hr\nabla^4$, and the forecast with $\approx 4hr\nabla^6$ respectively. It is clear that giving the forecast a more scale selective diffusion has had a beneficial impact on the forecast cyclone which now has a central pressure of 976hPa which is a significant improvement over 989hPa when compared to the analysis value of 961hPa. Clearly the forecast with the more scale selective diffusion has resulted in a more intense cyclogenesis and has improved the structure of the forecast cyclone. Indeed it can be seen from figure 12(d) that the contribution to the PV budget from horizontal diffusion for the forecast with the more scale selective diffusion has now been dramatically reduced. This confirms our hypothesis that the lack of scale selectivity of the diffusion was instrumental in destroying upper level PV and that this was a crucial element in the subsequent poor cyclogenesis in the forecast.

However, it should be noted that there remains deficiencies in the forecast cyclone (fig-

ure 12(c)) both in terms of intensity and position when compared to the analysis (figure 12(a)) or to the transplant experiments (figure 7(b)). This suggests that a lack of scale selectivity of the diffusion while significant, does not fully explain the poor forecast. Deficiencies in the initial analysis or in the model physics may also be playing an important role in the poor development of the forecast. There are also some unrealistic looking small scale features present in the PV plot shown in figure 12(e) and also in the horizontal diffusion plot (figure 12(d)) that suggests that the use of $4hr\nabla^6$ diffusion is contributing to numerical noise in the forecast.

The results of this study suggest that the present high levels of diffusion used in the operational model can have a significant impact on forecast cyclogenesis although, it is also clear that the scale selective diffusion used here is currently unsustainable. There are plans to change the operational model to have a semi-implicit semi-Lagrangian dynamical core (New Dynamics), which has an implicit diffusion, and may make it possible to use less explicit numerical diffision in the future. It is hoped that this will have a beneficial impact on mid-latitude cyclogenesis.

5 Conclusions

This report began by demonstrating systematic errors in the UM cyclogenesis in the Northern Hemisphere Atlantic Stormtrack region using both time mean Eulerian measures of error and also Lagrangian cyclone tracking diagnostics. Both the Eulerian and the Lagrangian diagnostics suggest that the model cyclogenesis is too weak in the west Atlantic and is too strong and stretches geographically too far to the east in the eastern Atlantic. In effect individual forecast cyclones have a tendency to deepen too slowly and weakly in the western Atlantic and fill too slowly and are too energetic in the eastern Atlantic.

The second part of this report has concentrated on various PV and Lagrangian trajectory diagnostic techniques along with sensitivity experiments in order to shed light on a particularly poor T+120 forecast from 15th Nov. 1998. The various techniques used in this study are.

- PV analysis of forecast and analysis using the Hoskins *et al* (1985) conceptual model of cyclogenesis.
- A PV transplant sensitivity experiment
- A Lagrangian trajectory package developed by Methven (1997) and using the coherent ensemble of trajectories approach of Wernli and Davies (1997) in order to track the differences in the flow of PV anomaly in the forecast and analysis.
- A PV budget equation approach in order to idenitify sources and sinks and total Lagrangian tendency of PV from model routine increments.
- A model physics sensitivity study in order to test the findings of the diagnostic study.

The basic approach has been to identify the problem using PV analysis and to use various diagnostic techniques to help reveal the source of the model deficiency and then to perform sensitivity experiment(s) in order to test conclusions.

This study suggested that for the case in question that the lack of scale selectivity and the high magnitude of the horizontal diffusion was important for the poor performance of this forecast. Without further work it is too early to suggest that horizontal diffusion contributes toward

the systematic error identified at the start of this report. While this single case study cannot be taken as a conclusive result, it is suggested that the diagnostic approach and techniques demonstrated here are useful in helping to identify the cause of model error in the stormtracks and could be applied to more cases in the future.

References

Anthes, A. E., 1983: Numerical simulations of a case of explosive marine cyclogenesis. *Mon. Wea. Rev.*, **111**, 1174–1188.

Hoskins, B. J., M. E. McIntyre, and A. W. Robertson, 1985: On the use and significance of isentropic potential vorticity maps. *Q. J. R. Met. Soc.*, **111**, 877–946.

Klinker, E., 1994: Diagnosis of Diabatic Processes. *Parametrization of sub-grid scale physical processes*, ECMWF Seminar Proceedings, 357–371.

Methven, J., 1997: Offline Trajectories: Calculation and Accuracy. UGAMP Technical Report 44, UGAMP.

Rabier, F., E. Klinker, P. Courtier, and A. Hollingsworth, 1996: Sensitivity of forecast errors to initial conditions. *Q. J. R. Met. Soc.*, **122**, 121–150.

Stoelinga, M., 1996: A PV based study of the role of diabatic heating and friction in a numerically simulated baroclinic cyclone. *Mon. Wea. Rev.*, **124**, 849–874.

Terry, J., and R. Atlas, 1996: Objective cyclone tracking and its application to ERS-1 scatteromter forecast impact studies. *AMS 15th Conference on Weather and Forecasting.*, Norfolk, Virgina, US, 146–149.

Wernli, H., and H. C. Davies, 1997: A Lagrangian-based analysis of extratropical cyclones. I: The method and some applications. *Q. J. R. Met. Soc.*, **123**, 467–489.

Wirth, V., and J. Egger, 1999: Diagnosing extratropical synoptic-scale stratosphere-troposphere exchange: A case study. *Q. J. R. Met. Soc.*, **125**.

List of Figures

a) Analysis

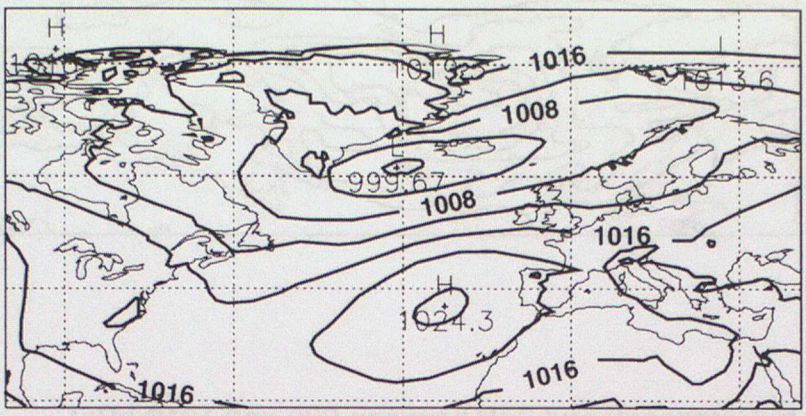

b) T+120 Forecasts

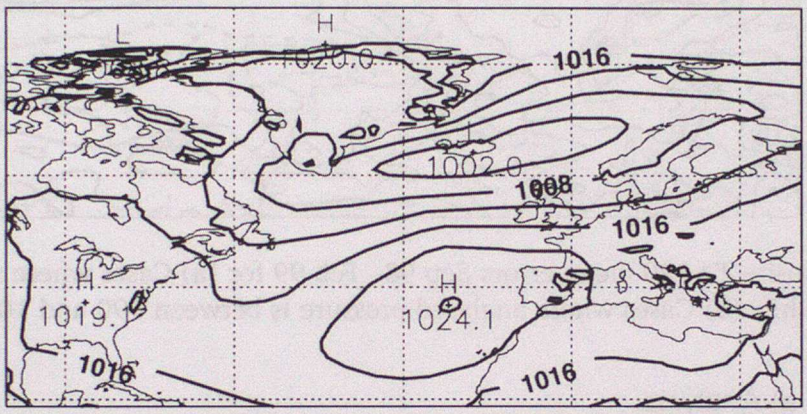

c) Mean Error T+120

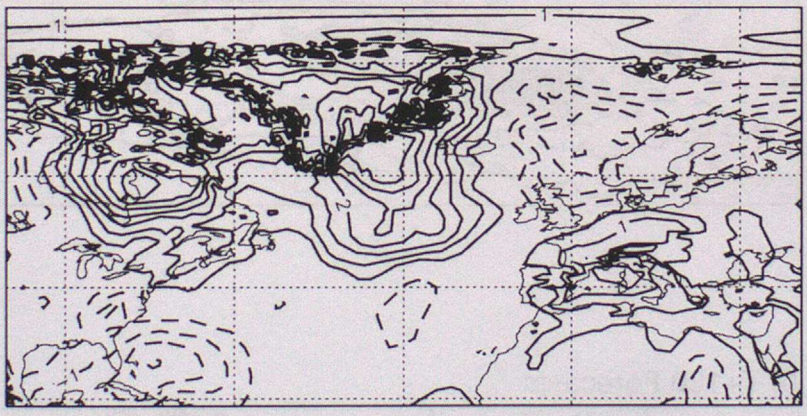

d) Random Error T+120

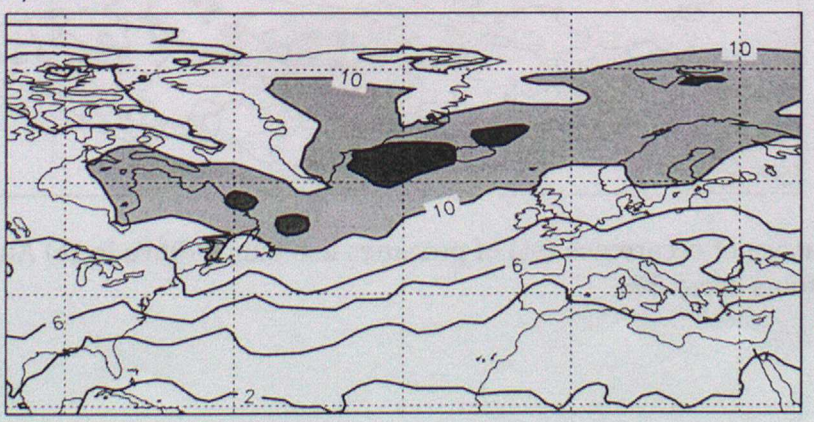

Figure 1: Time mean MSLP Sept 98 - Feb 99. a) Analysis, b) T+120 forecasts, c) Mean error at T+120 d) Error standard deviation

a) Category 1 (P less than 990 hPa)

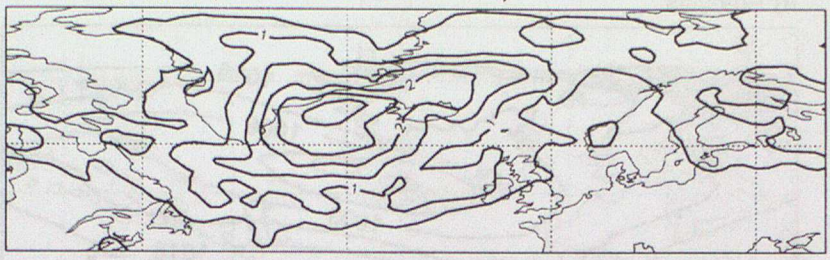

b) Category 2 and 3 (P between 990 and 1010 hPa)

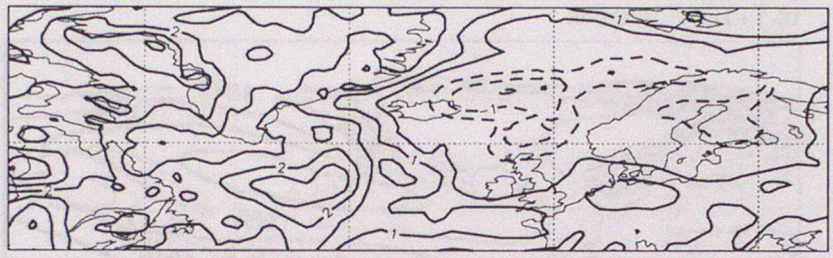

Figure 2: Composite T+120 mean errors Sep 98 - Feb 99 for (a) Cases where analysed pressure is less than 990 hPa (b) Cases where analysed pressure is between 990 and 1010 hPa. Contours every 0.5 hPa.

a) Analysis

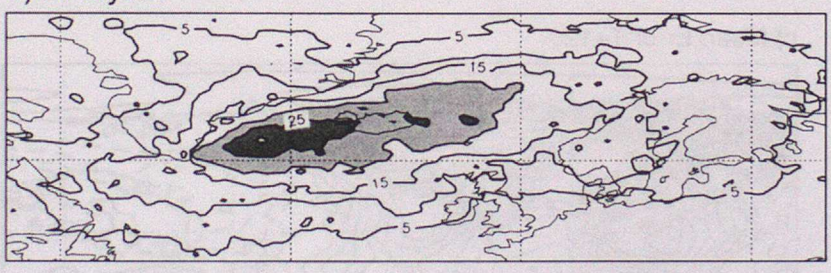

b) T+120 Forecasts

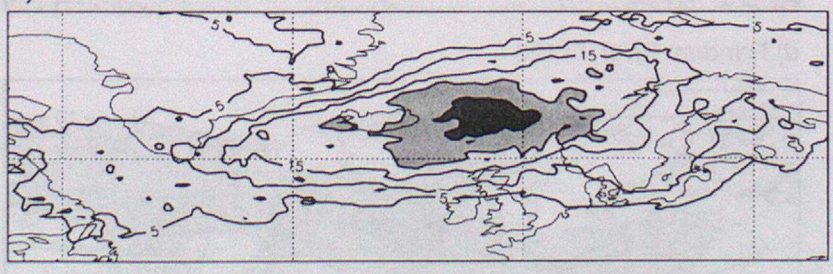

Figure 3: Frequency of occurrence (%) of pressures less than 990hPa in (a) Analysis, (b) T+120 Forecasts. Contours every 5%

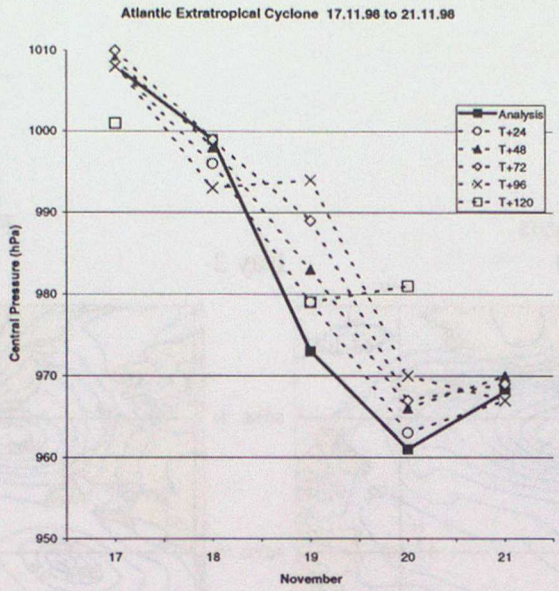

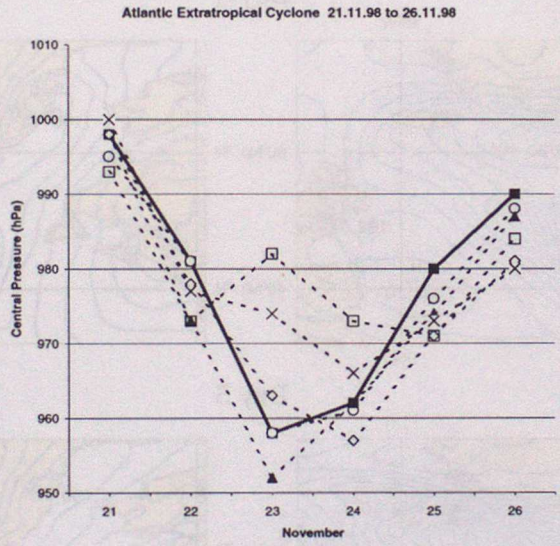

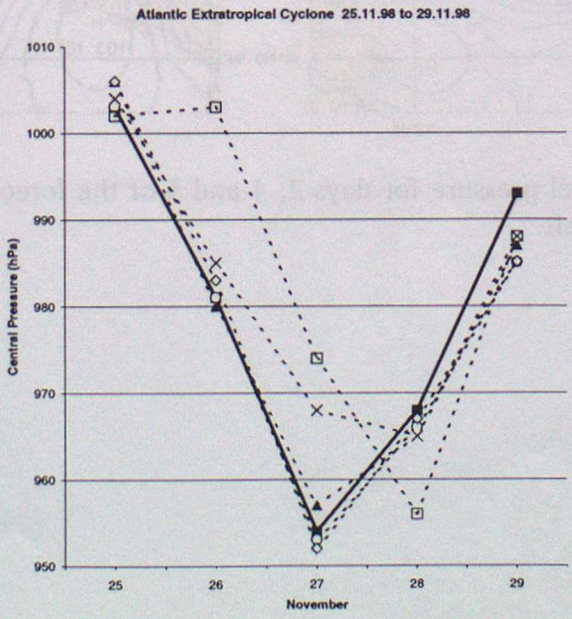

Figure 4: Central pressures of three Atlantic extratropical cyclone events. a) 17-21 Nov 98, b) 21-26 Nov 98, c) 25-29 Nov 98.

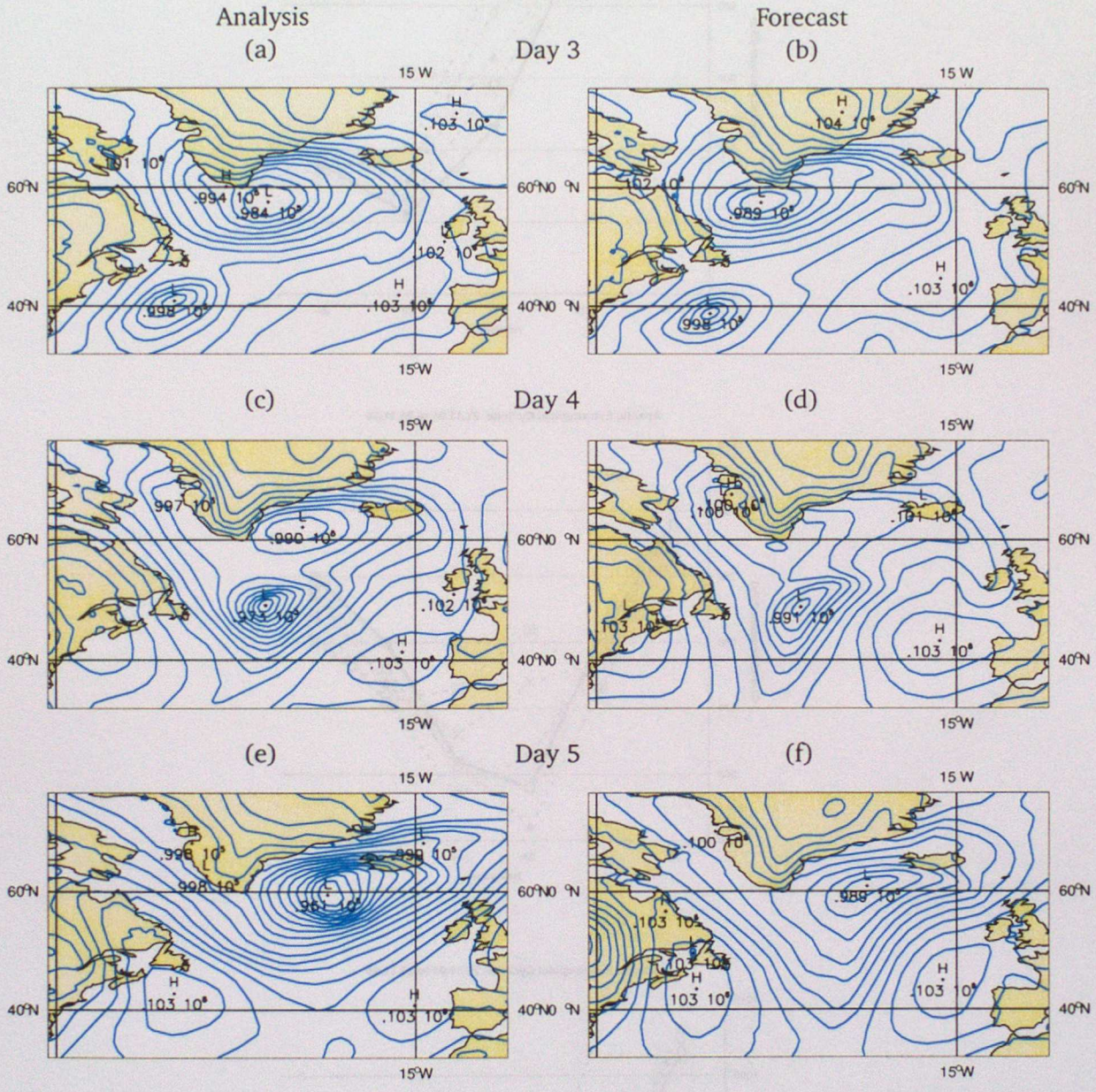

Figure 5: Mean sea level pressure for days 3, 4 and 5 of the forecast with the corresponding analyses shown to the left.

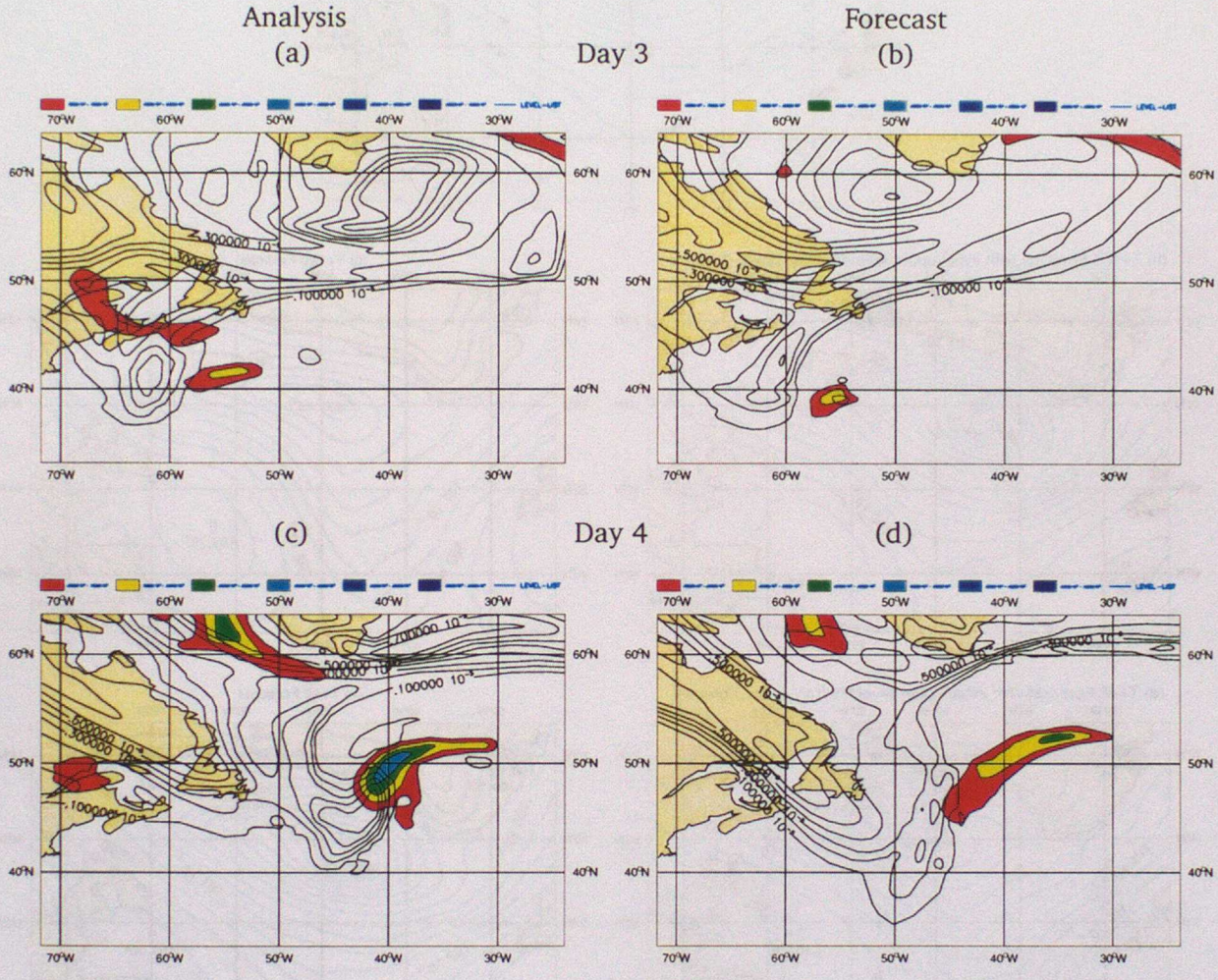

Figure 6: For days 3 and 4 of the forecast and corresponding analyses to the left, are shown 315K Ertel PV in bold contours and 850hPa Potential Vorticity in colour filled contours. The first colour filled contour is from 0-1PVU and then increments by 0.5PVU subsequently.

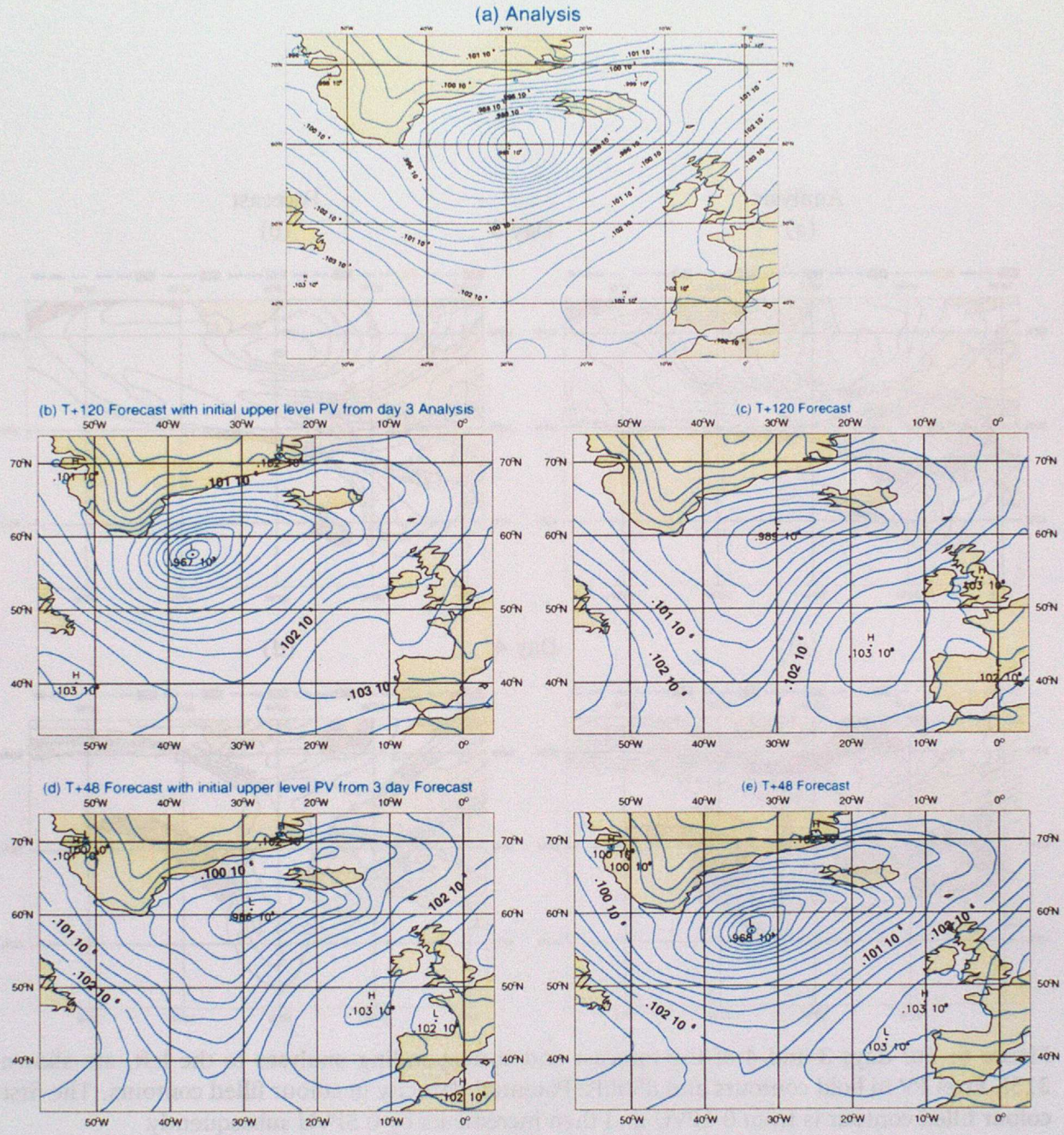

Figure 7: Mean sea level pressure charts for 20/11/98 (experiment names which refer to a table in the text are shown in brackets) (a) Analysis at 20/11/98 (b)(TRA120) T+120 Forecast with upper level PV transplanted from an analysis at T+72 (c)(CTL120) T+120 Forecast from 15/11/98 (d)(TRF48) T+48 Forecast from 18/11/98 with upper level PV from a T+72 forecast started at 15/11/98 (e)(CTL48) T+48 Forecast from 18/11/98.

(a)

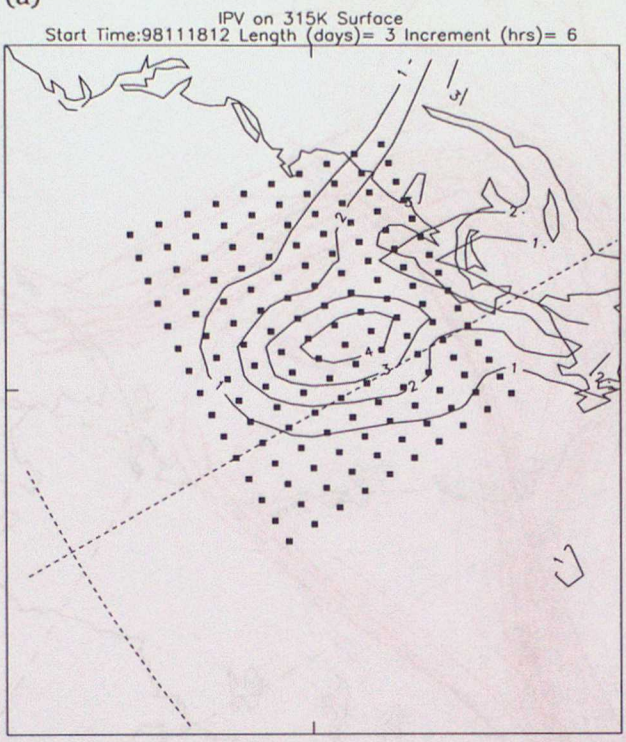

(b)

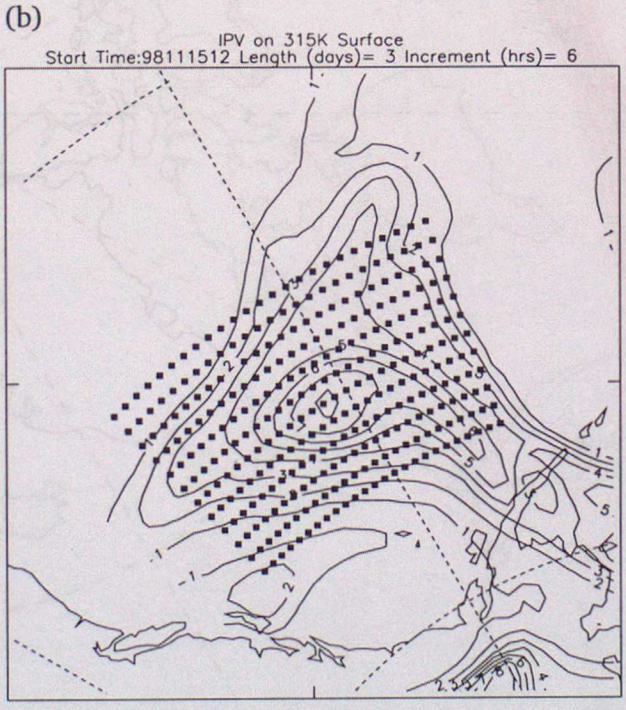

Figure 8: Dots mark the starting positions of (a) backward (situated off the east coast of America) or (b) forward trajectories (situated just south of Alaska). Contours are of Ertel PV on the 315K surface from (a) an analysis at 18/11/20 and (b) an analysis at 15/11/98.

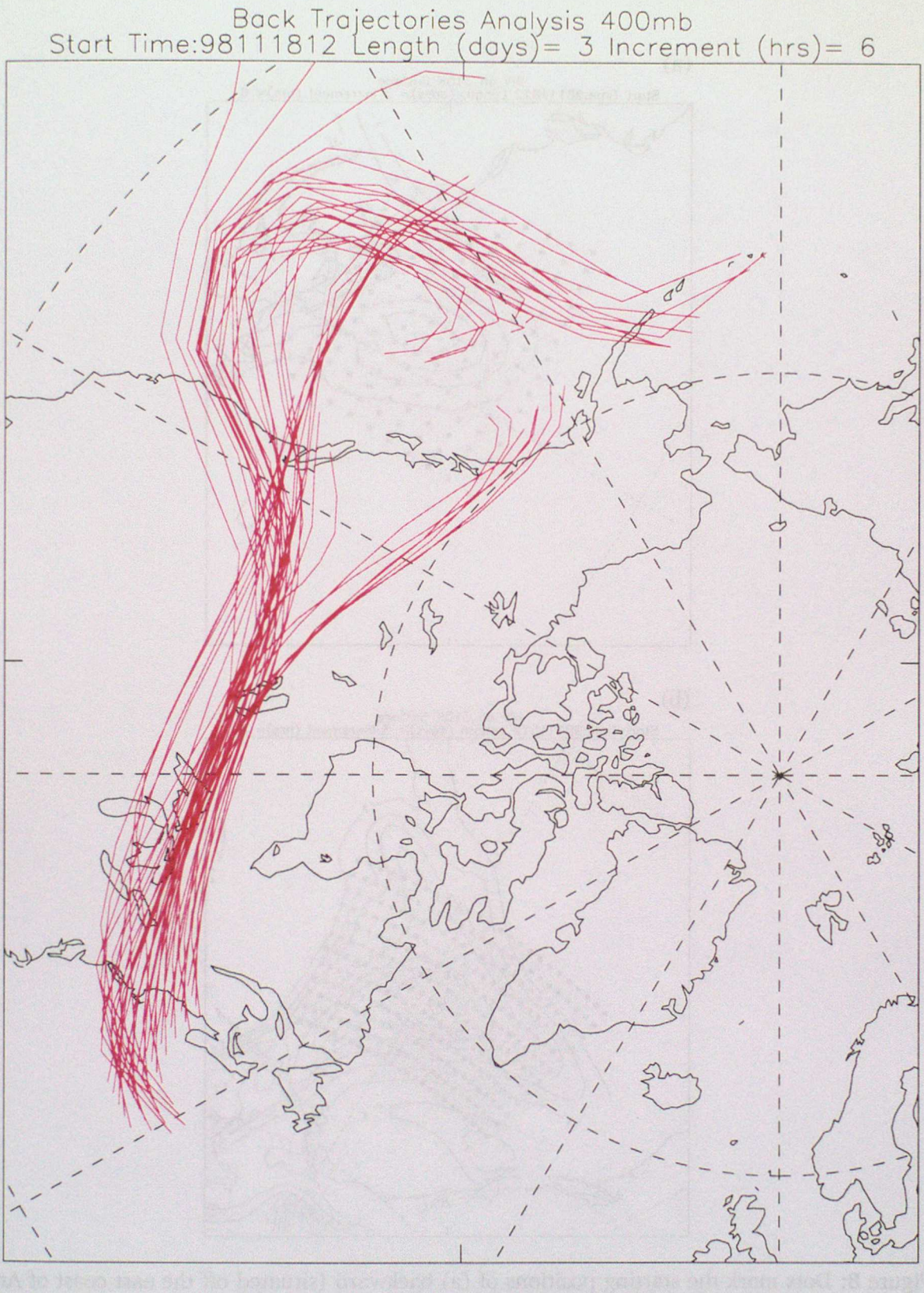

Figure 9: Plot shows 72 hour backward trajectories for parcels from an analysis at 18/11/98 starting at positions shown in figure 8(a) and at a height of 400hPa. The trajectories shown were selected to have a value of PV greater than 1PVU at 400hPa at their starting positions.

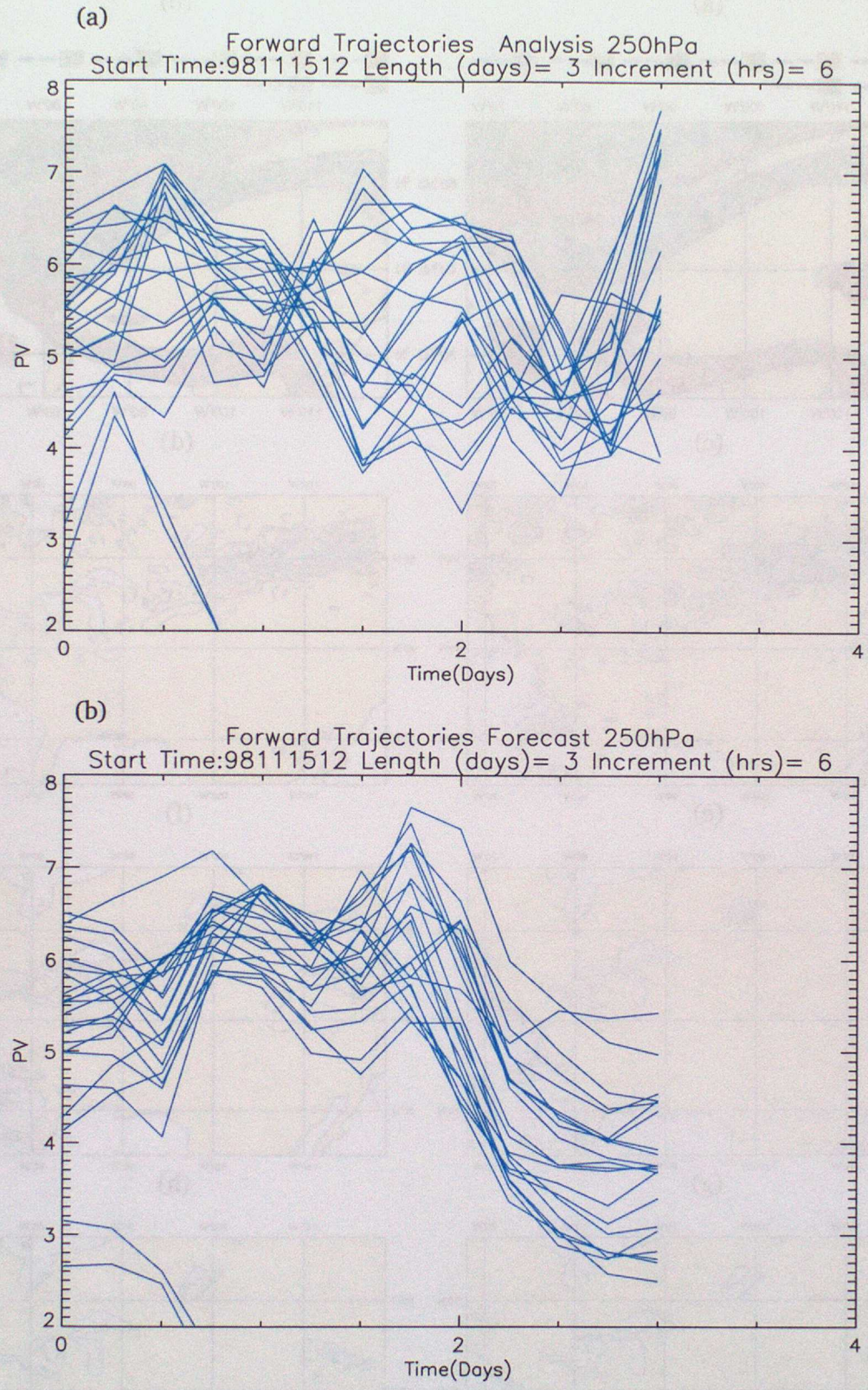

Figure 10: Plots show 72 hour forward trajectories from an analysis at 12z on 15/11/98 starting at positions shown in figure 8(b) and at a height of 250hPa. Shown in (a) are analysis trajectories chosen to end up in the region depicted by the dots in figure 8(a) and (b) forecast trajectories which are chosen to have the same starting positions as the selected analysis ones.

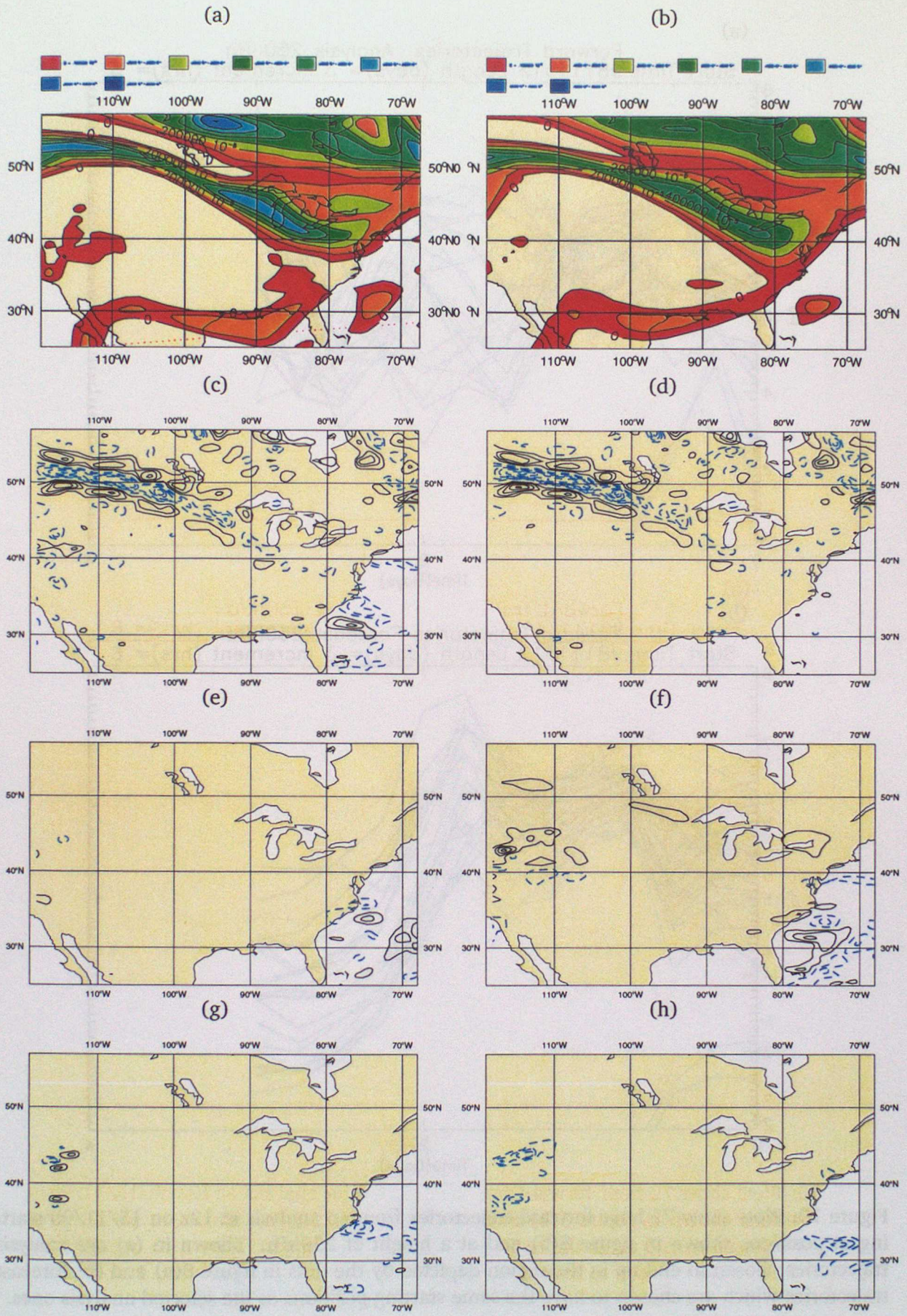

Figure 11: Shown in (a) and (b) is PV at 300hPa for the analysis and forecast after 42 hours. The first contour interval is 0-1PVU and then increments by 0.5PVU. Shown in (c) is the total Lagrangian dervivative of PV, (d) is the contribution to (c) from horizontal diffusion, (e) is from conv. momentum, (f) is from LW, (g) is from convection and (h) is from latent heating. (c) to (h) are calculated using a PV budget equation described in the text for the period 36-42 hrs at 300hPa. Blue dashed contours denote negative values and the contour interval is 5E-12.

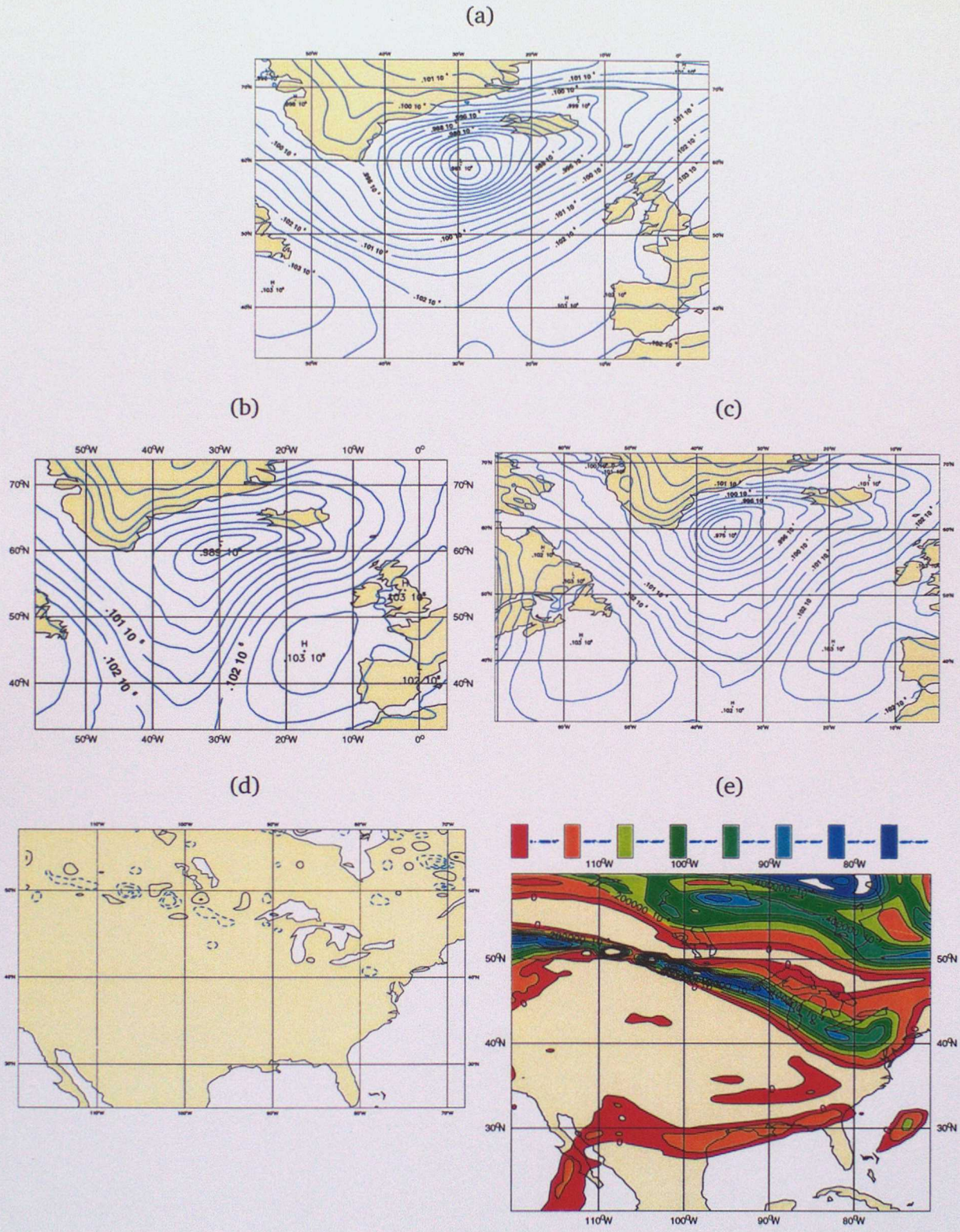

Figure 12: Shown in (a), (b) and (c) is mslp for the analysis on the 20/11/98, the corresponding T+120 forecast with ∇^4 diffusion and a forecast with ∇^6 diffusion respectively. Shown in (c) and (d) are diagnostics described in figure 11(d) and (b) respectively for a forecast with ∇^6 diffusion.